Opportunistic Robot Control for Interactive Multiobjective Optimization under Human Performance Limitations

Pio Ong [a] Jorge Cortés [a]

[a] *Department of Mechanical and Aerospace Engineering, University of California, San Diego, {piong,cortes}@ucsd.edu*

Abstract

This paper proposes opportunistic state-triggered strategies for solving convex multiobjective optimization problems that involve human-robot interaction. The robot is aware of the multiple objective functions defining the problem, but requires human input to find the most desirable Pareto solution. In order to avoid overloading the human with queries, we view her as a limited resource to the robot, and design event-triggered controllers that opportunistically prescribe the information exchanges among them. We consider various models of human performance, starting with an ideal one where queries are responded instantaneously, and later considering constraints on the response time and the interaction frequency. For each model, we formally establish the asymptotic convergence to the desired optimizer and rule out the existence of Zeno behavior.

Key words: Event-triggered control, multiobjective optimization, multiple criteria decision making, human-robot interaction.

1 Introduction

In the not so distant future, it is envisioned that robots will cooperate with humans in performing a multitude of tasks in everyday life, ranging from routine jobs to dangerous missions. This paper is motivated by this vision, and considers scenarios where a robot is faced with balancing the satisfaction of multiple objectives and resorts to a human supervisor to assess the various trade-offs in doing so. As an illustration, consider a motion planning problem where the robot seeks to find a shortest path between origin and destination while staying away from various undesired locations that may contain adversaries of varying threat levels. As information is learned about the environment, a human can assist the robot in assessing the threat levels. This type of cooperation, when done reliably and efficiently, can lead to higher degrees of performance and adaptiveness in the resulting robot behavior. To manage the human workload required by this cooperation, we take a resource-aware control design viewpoint, where the human is regarded as a resource whose used by the robot is not unlimited. We are interested in understanding to what extent constraints in human performance, such as response time to queries and frequency of queries, can be accommodated in the robot executions while still guaranteeing the convergence to the desired optimal solution of the multiobjective optimization.

Literature review. We rely on three bodies of literature: multiobjective optimization, human-robot interaction and event-triggered control. Interactive approaches in multiobjective optimization involve an algorithmic strategy that "interacts" with a human supervisor to determine an acceptable solution to the problem A comprehensive survey on interactive approaches can be found in [Miettinen et al., 2008], which groups different techniques into three main categories: the trade-off approach, the reference points approach, and the classification method. Algorithmic solutions often combine elements of several of these categories. In the scenarios considered here, the optimization problems arise as the human-robot system explore the world, and hence global information is not available a priori. Most works in the trade-off approach focus on finding local information, usually related to the gradient of an implicit preference function at each iteration that ranks different outcomes [Geoffrion et al., 1972, Sakawa, 1982, Yang, 1999]. The implicit preference function is well-studied and utilized in utility theory. For example, its existence is proven in an important result in [Debreu, 1954] under mild assumptions. Using an implicit preference function is common for solving a multiobjective problem, see e.g., [Geoffrion et al., 1972, Luque et al., 2009, Miettinen et al., 2008]. We follow this idea when proposing our results. The above reference list is relatively old because newer methods often require global information, such as the knowledge of the optimizer of each objective function or the knowledge of the Pareto front. For a list of newer methods with brief summaries of them, we refer the readers to [Xin et al., 2018].

The literature of human-robot interaction has become vast with the accelerated pace of development in robotics. A good overview is captured by the survey [Goodrich and Schultz, 2007]. Our work can be classified under the category of supervisory control. One of the many human factors often explored in the human-robot interaction is the amount of workload on the human, see e.g., [Peters et al., 2015, Steinfeld et al., 2006]. An important concept is neglect time and interaction time as presented in [Crandall et al., 2005]. Closely related is the concept of response and reaction time, which becomes important when the human needs to work and respond to robots in the real world [Har-

⋆ This work was supported by NSF Award ECCS-1917177.
A preliminary version of this paper appeared at the IEEE Conference on Decision and Control as [Ong and Cortés, 2017].

riott and Adams, 2017]. To accommodate these time factors, we employ techniques from event-triggered control, see [Heemels et al., 2012, Miskowicz, 2015, Tabuada, 2007, Wang and Lemmon, 2011] and reference therein for great introductions to the topic. Event-triggered control has shown success in improving efficiency on the use of system resources across actuation, sensing, communication, and computing. Of particular relevance to the topic here are works that employ the event-triggered design approach in the context of optimization, usually in distributed settings where communication among agents is viewed as a limited resource, see e.g., [Kia et al., 2015, Richert and Cortés, 2016, Wang and Lemmon, 2011, Weimer et al., 2012]. The application of resource-aware ideas to a multiobjective optimization setting, with the human as the resource available to the robot whose use should be minimized, are novel aspects of this paper. In dealing with time constraints, we utilize the flexibility of event-triggered control to deal with delay, see e.g., [Dolk et al., 2017, Hetel et al., 2006, Li et al., 2012, Wu et al., 2015]. Although the results there are not directly applicable to our presented problem because of the particular features of the human-robot setup, we follow the idea of bounding interevent times to deal with delay, cf. [Li et al., 2012, Tabuada, 2007]. In addition, we also employ the novel idea in event-triggered control of allowing the certificate function to increase along trajectories. This idea can be found in dynamic triggering [Dolk et al., 2014, Girard, 2015] and in designs based on performance barrier triggering [Ong and Cortés, 2018], and allows us to consider more general constraints on human performance.

Statement of contributions. We consider a convex multiobjective optimization problem where a robot works alongside a human to find a Pareto optimal solution. Based on its knowledge of the multiple objective functions, the robot presents outcomes to the human, who expresses her preference among them. The human cannot express in closed form the function she uses to evaluate the outcomes, but can provide its gradient (this is a convenient abstraction of the ability of the human to express preferences about an outcome being better than another). Throughout the paper, we consider models of increasing complexity about how the human can interact with the robot. Our contributions are multiple fold. Our first contribution considers the ideal case, where the human can respond instantaneously to the robot queries. We propose an event-triggered design that allows the robot to interact with the human in an opportunistic fashion as required by the solution of the overarching multiobjective optimization problem, thereby reducing human workload. Our design is based on examining the evolution of the value of the outcomes along the robot trajectories and ensuring that it is decreasing. We next move on to consider timing constraints on human performance. Our second contribution considers the "need to rest" case, where the human needs some time after responding to a query before she can respond to a new one. In effect, this means that the robot might not get the information it requires if two queries are formulated in quick succession. We examine to what extent our original trigger design case can be made valid for this case by tuning a design parameter and characterize the human resting times that can be tolerated. To accommodate longer resting times, we propose an alternative trigger design that allows the certificate to increase at times during the evolution, as long as it decreases when evaluated at consecutive human's queries. To do this, our technical treatment introduces the important concepts of critical time and grace period. Critical time refers to how long without human input and by how much the robot can guarantee the monotonic decrease of the certificate. After the critical time, grace period refers to the amount of time the robot can still wait without querying the human while the certificate potentially increases, but not beyond the value it had when information was last received from the human. We show that this design can accommodate longer resting times than our original design. Our third contribution considers the "need to think" case, where the human needs some time before responding to a query. Our design is based on the robot anticipating the evolution of the certificate for the period of time the human may take in responding, and using this information to query the human sufficiently in advance by tuning appropriately a design parameter in our original design. Finally, our last contribution considers the model of human performance that combines both "need to rest" and "need to think" timing constraints. For each model, we provide a complete analytical treatment of the proposed design that includes establishing the monotonic decrease of the certificate, a uniform lower bound on the minimum time between consecutive queries (thereby ruling out Zeno behavior), and the asymptotic correctness of the resulting algorithm to the desired optimal solution. Throughout the paper, we provide explicit expressions of the lower bounds on the minimum interevent time which, together with the characterization of the convergence rates of the dynamics, provide a mean to assess the trade-offs between the frequency of human queries and the algorithm performance. Simulations on an example in multiobjective robot motion planning show the reductions in human workload obtained by the proposed event-triggered design versus algorithms that require continuous human involvement. We also illustrate the trade-offs between design convergence rate, human workload, and human response time.

Notation. For $n \in \mathbb{N}$, we let $[n] = \{1, \dots, n\}$. Given $x \in \mathbb{R}^n$ and $A \in \mathbb{R}^{m\times n}$, $\|x\|$ and $\|A\|$ denote Euclidean and spectral norm, respectively. We use $I_n \in \mathbb{R}^{n\times n}$ for the identity matrix. Given $f : \mathbb{R}^n \to \mathbb{R}^m$, $f_i : \mathbb{R}^n \to \mathbb{R}$ denotes its ith-component. f is Lipschitz on $\mathcal{S} \subset \mathbb{R}^n$ if there exists $L > 0$, termed Lipschitz constant, such that $\|f(x) - f(y)\| \leq L\|x - y\|$, for all $x, y \in \mathcal{S}$. For a continuously differentiable f, $J_f : \mathbb{R}^n \to \mathbb{R}^{m\times n}$ denotes its Jacobian matrix. For f and $g : \mathbb{R}^m \to \mathbb{R}$, the composition of functions is $g\circ f : \mathbb{R}^n \to \mathbb{R}$, i.e., $(g \circ f)(x) = g(f(x))$ for $x \in \mathbb{R}^n$. For a twice continuously differentiable, scalar-valued function $g : \mathbb{R}^n \to \mathbb{R}$, we let $\nabla g : \mathbb{R}^n \to \mathbb{R}^n$ and $\nabla^2 g : \mathbb{R}^n \to \mathbb{R}^{n\times n}$ denote its gradient and Hessian functions. g is convex on $\mathcal{S}$ if, for all $x \in \mathcal{S}$, $\nabla^2 g(x) \succeq 0$; strictly convex if $\nabla^2 g(x) \succ 0$; and strongly convex if there exists $\mu > 0$ such that $\nabla^2 g(x) \succeq \mu I_n$. If g is strongly convex on $\mathcal{S}$, its sublevel sets contained in $\mathcal{S}$ are bounded. This implies that there exists $M > 0$ such that $\nabla^2 g \preceq M I_n$ on $\mathcal{S}$. In fact, if x^* is the minimizer of g, then

$$\frac{1}{2M}\|\nabla g(x)\|^2 \leq g(x) - g(x^*) \leq \frac{1}{2\mu}\|\nabla g(x)\|^2. \quad (1)$$

2 Interactive Multiobjective Optimization

Consider a human-robot system that seeks to find the minimizer to a vector-valued, continuously differentiable function, function $f : \mathbb{R}^n \to \mathbb{R}^m$, i.e. $\min_{x\in\mathbb{R}^n} f(x)$. Each of the components of f represents a goal the robot is trying to achieve, and x represents the decision variable. A point $x_{\rm po} \in \mathbb{R}^n$ is a solution to the minimization problem if there does not exist $x \in \mathbb{R}^n$ with $f_i(x) \leq f_i(x_{\rm po})$ for all $i \in [m]$ with at least one inequality being strict. These solutions, called Pareto points, capture the fact that improving the minimization of one component of f cannot be done without increasing the value of another. In principle, there exist multiple Pareto points corresponding to the different tradeoffs in optimizing the components of f.

Many multiobjective optimization problems find applications in practical scenarios involving control formulations, cf. [Peitz and Dellnitz, 2018]. Usually, the decision variable corresponds to the control input. For example, [Peitz et al., 2017] considers an MPC formulation in autonomous driving where the control u can affect both the arrival time and energy consumption. When doing motion planning, the robot must consider the different conflicting factors involved, see [Shaikh and Goodrich, 2017].

2.1 Interactive Approach

In general, finding the whole set of Pareto points is computationally expensive. Furthermore, additional considerations might make some Pareto points more desirable than others. One way to address this is via the interactive approach, where a human is involved in determining the desirable outcome. This has the added benefits of reduction in computational resource usage, improved desirability of the obtained solution, and adaptability to different scenarios.

Consider the following human-robot model. The robot has first-order fully actuated dynamics and is assumed to have knowledge of the component objective functions in f. A human operator assists the robot in selecting the most appropriate Pareto point. As is commonly done in trade-off approaches to multiobjective optimization problems, we assume the human has a scalar-valued, continuously differentiable function $v : \mathbb{R}^m \to \mathbb{R}$ that ranks the different outcomes, i.e., $v(f(x))$ represents the 'value' that the human gives to the outcome $f(x)$ achieved at $x \in \mathbb{R}^n$. This function can then be used to establish a preference among all Pareto points. However, the function v is implicit, meaning that the human does not know it in closed form, but can respond to queries about it. Specifically, we model the human as being able to express preferences about an outcome being better than another one, and we abstract this with gradient information of v: if the robot queries the human about its current value $f(x)$, the human can provide the value $\nabla v(f(x))$, indicating the direction of change in which outcomes are more highly valued.

The optimization problem consists of maximizing $v \circ f$. For convenience, we instead formulate it as a minimization problem by considering the cost function $c = -v$. The problem to solve is then $\min_{x\in\mathbb{R}^n}(c \circ f)(x)$. We assume the composition function $c \circ f$ is strictly convex, and that the problem has a unique minimizer x^*, which we can find via the gradient descent algorithm

$$\dot{x} = -\nabla(c \circ f)(x)^\top = -(\nabla c(f(x))J_f(x))^\top,$$

which globally asymptotically converges to x^*. This can be shown by considering the value of $c \circ f$, which strictly decreases over time along the trajectory. Note, however, that the implementation of the gradient dynamics by the robot is problematic. The robot knows the objective function f and can therefore compute its Jacobian, J_f. However, $\nabla c \circ f$ can only be provided by the human because only she knows the cost function. Therefore, executing the dynamics would require the human to continuously relay preference information to the robot, which is not feasible. The discretization of the dynamics with a constant stepsize would make its implementation plausible, albeit it still requires constant, periodic human involvement. Given that the stepsize needs to be sufficiently small to guarantee convergence for arbitrary initial conditions, this may still impose an unnecessary burden on the human. The basic premise of the paper to tackle this is to endow the robot with criteria that allow it to determine, in an opportunistic fashion, when to query the human to avoid her unnecessary involvement.

2.2 Problem Statement

Motivated by Section 2.1, we consider the following gradient dynamics, which discretizes the human component but maintains the continuous evolution of the robot component,

$$\dot{x} = -(\nabla c(f(x_k))J_f(x))^\top, \quad t_k \leq t < t_{k+1}, \tag{2}$$

where x_k is shorthand notation to represent $x(t_k)$. Under this dynamics, the human operator only needs to assess the robot performance at the time instants $\{t_k\}_{k=0}^\infty$. Our goal in this paper is to design triggers that the robot can evaluate on its own to determine this sequence of times efficiently, while still guaranteeing the asymptotic convergence to the desired solution and the feasibility of the resulting implementation (i.e., interevent times are uniformly lower bounded and hence the implementation is free of Zeno behavior). What makes the trigger design and analysis different from other event-triggered control formulations is that the resource to be aware of here is the human. In particular, the fact that the preference function c is unknown to the robot (even the human does not explicitly know it, as discussed above) and the various human behaviors (e.g., unable to comply with multiple rapidly succeeding requests for information) detailed later in Sections 3 and 4 rule out the use of standard results in event-triggered control.

In this paper, we consider different models for human behavior, starting with an ideal model where the human can respond instantaneously. We then move to consider models with timing constraints, such as when the human needs time to rest between queries, may take time to respond to a query, or a combination thereof. For each model, we propose a trigger design that satisfies the above criteria.

Remark 2.1 (Strict Convexity of the Composition Function). Note that, if all the component functions of f are strictly convex and the cost function c is both strictly increasing in each component (which is reasonable, given that the human seeks to minimize each individual component) and strictly convex, then $c \circ f$ is also strictly convex. •

3 Event-Triggered Design: Ideal Human

Here we synthesize a triggering condition for the robot that allows it to efficiently query the human about her preferences on the optimization of the vector-valued objective function. We assume that the human performance is ideal, meaning that the human can respond to queries immediately, i.e., there is no delay in obtaining the value of $\nabla c \circ f$.

Our trigger design is based on analyzing the evolution of the cost function evaluated on the objectives towards its optimal value. We consider

$$V(x) = c(f(x)) - c(f(x^*)). \tag{3}$$

Note that V is radially unbounded and has compact sublevel sets due to our assumptions on strict convexity and existence of a unique minimizer. For convenience, we use the shorthand notation $w = \nabla c \circ f : \mathbb{R}^n \to \mathbb{R}$, and, for $k \in \{0\} \cup \mathbb{N}$ and $t \geq t_k$, we let $\Delta x_k = x(t) - x_k$ denote the error between the state at time t and the state when the gradient was last updated at time t_k. The next result identifies a gradient update triggering condition that ensures V decreases on a neighborhood of the optimizer.

Proposition 3.1 (Trigger for Ideal Human). *Consider the event-triggered human-robot system* (2) *and let $x_k \neq x^*$ be the state when the gradient information was last updated. Let $\mathcal{V} \subseteq \mathbb{R}^n$ be a neighborhood of the optimizer such that $x_k \in \mathcal{V}$ and let L_c be the Lipschitz constant of $\nabla c \circ f$ over $\mathcal{V}$. For $\sigma \in (0, 1]$, let t_{k+1} be determined by*

$$t_{k+1} = \min\left\{ t \geq t_k \mid \|\Delta x_k\| = \frac{\sigma \|\nabla c(f(x_k)) J_f(x)\|}{L_c \|J_f(x)\|} \right\}. \tag{4}$$

If $\mathcal{S}_k = \{x \in \mathbb{R}^n \mid V(x) \leq V(x_k)\} \subseteq \mathcal{V}$, then for all $t \in [t_k, t_{k+1})$, we have

$$\frac{d}{dt} V(x(t)) < -\frac{1-\sigma}{(1+\sigma)^2} \|\nabla c(f(x(t))) J_f(x(t))\|^2. \tag{5}$$

PROOF. First we note that V is positive definite because x^* is unique. Let $\Delta w_k = w(x) - w(x_k)$. Then the time derivative of V at $t \in [t_k, t_{k+1})$ is

$$\begin{aligned}
\frac{d}{dt} V(x(t)) &= (w(x) J_f(x))\dot{x} = -(w(x) J_f(x))(w(x_k) J_f(x))^\top \\
&= -((w(x_k) + \Delta w_k) J_f(x))(w(x_k) J_f(x))^\top \\
&\leq -\|w(x_k) J_f(x)\|^2 \\
&\quad + \|\Delta w_k\| \|J_f(x)\| \|w(x_k) J_f(x)\| \\
&\leq -\|w(x_k) J_f(x)\|^2 \\
&\quad + L_c \|\Delta x_k\| \|J_f(x)\| \|w(x_k) J_f(x)\|.
\end{aligned}$$

The last inequality relies on the assumption that w is Lipschitz on $\mathcal{S}_k$ with constant L_c so that $\|\Delta w_k\| \leq L_c \|\Delta x_k\|$. Since $\|\Delta x_k\| = 0$ at time t_k, and given the definition (4) of t_{k+1}, we have $\|\Delta x_k\| < \sigma\left(\frac{\|\nabla c(f(x_k)) J_f(x)\|}{L_c \|J_f(x)\|}\right)$ on the interval $[t_k, t_{k+1})$. We can then deduce that

$$\frac{d}{dt} V(x(t)) < -(1-\sigma) \|w(x_k) J_f(x(t))\|^2. \tag{6}$$

This shows that $\frac{d}{dt} V(x(t))$ is negative, and hence the set $\mathcal{S}_k$ is invariant under (2). Next, we find a relationship between $\|w(x) J_f(x)\|$ and $\|w(x_k) J_f(x)\|$ as follows,

$$\begin{aligned}
\|w(x) J_f(x)\| &\leq \|w(x_k) J_f(x)\| + \|\Delta w_k J_f(x)\| \\
&\leq \|w(x_k) J_f(x)\| + L_c \|\Delta x_k\| \|J_f(x)\| \\
&< (1+\sigma) \|w(x_k) J_f(x)\|,
\end{aligned} \tag{7}$$

where we have again used the bound on $\|\Delta x_k\|$ from the design to bound the last inequality. The result now follows by substituting (7) into (6). □

Note that the hypothesis that $\mathcal{S}_k \subseteq \mathcal{V}$ is easily satisfied given that V is radially unbounded. Proposition 3.1 provides a trigger design (4) under which the function V is strictly monotonically decreasing. One important feature of the trigger design is that the design only relies on $\nabla c(f(x))$ at $x = x_k$, which is available to the robot. This ensures that the monitoring of this condition can be evaluated during each iteration independently by the robot, i.e., the human is only queried at discrete instants of time. Nevertheless, we cannot yet conclude that the optimizer is asymptotically stable. The reason for this is that we first need to discard Zeno behavior, i.e., the possibility of (4) inducing an infinite number of trigger updates in a finite amount of time. To do so, it is useful to characterize how the system state discretization error, $\|\Delta x_k\|$, evolves during interexecution periods, i.e., between consecutive updates, independently of how triggering times are determined.

Lemma 3.2 (State Deviation Bound). *Consider the event-triggered human-robot system* (2) *and let x_k be the state when the gradient information was last updated. For any triggering time t_{k+1} such that $x(t) \in \mathcal{S}_k$ for all $t \in [t_k, t_{k+1})$, the system state discretization error satisfies*

$$\|\Delta x_k\| \leq \phi_k(t - t_k) \|\dot{x}\| \tag{8}$$

during the interexecution period $[t_k, t_{k+1})$, where $\phi_k(t) = \frac{1}{M_k}(e^{M_k t} - 1)$ with $M_k = \max_{x \in \mathcal{S}_k} \|\nabla^2(w(x_k) f(x))\|$.

PROOF. We first note that the case where $x_k = x^*$ is trivial. Then for $x_k \neq x^*$, we must have that $\dot{x} \neq 0$ at time t_k and we can examine the dynamics of $\|\Delta x_k\| / \|\dot{x}\|$.

$$\begin{aligned}
\frac{d}{dt} \frac{\|\Delta x_k\|}{\|\dot{x}\|} &= \frac{d}{dt} \frac{(\Delta x_k^\top \Delta x)^{1/2}}{(\dot{x}^\top \dot{x})^{1/2}} \\
&= \frac{(\Delta x_k^\top \Delta x_k)^{-1/2} \Delta x_k^\top \dot{\Delta x}_k (\dot{x}^\top \dot{x})^{1/2}}{\dot{x}^\top \dot{x}} \\
&\quad - \frac{(\dot{x}^\top \dot{x})^{-1/2} \dot{x}^\top \ddot{x} (\Delta x_k^\top \Delta x_k)^{1/2}}{\dot{x}^\top \dot{x}} \\
&= \frac{\Delta x_k^\top \dot{\Delta x}_k}{\|\Delta x_k\| \|\dot{x}\|} - \frac{\dot{x}^\top \ddot{x} \|\Delta x_k\|}{\|\dot{x}\|^3} \\
&\leq \frac{\|\Delta x_k\| \|\dot{\Delta x}_k\|}{\|\Delta x_k\| \|\dot{x}\|} + \frac{\|\dot{x}\| \|\ddot{x}\| \|\Delta x_k\|}{\|\dot{x}\|^3} = 1 + \frac{\|\Delta x_k\|}{\|\dot{x}\|} \frac{\|\ddot{x}\|}{\|\dot{x}\|},
\end{aligned} \tag{9}$$

where in the last step we have used the fact that $\dot{\Delta x}_k = \dot{x}$. Now, we define the function $V_k(x) = w(x_k) f(x)$, and write

$$\ddot{x} = \frac{d}{dt}(-w(x_k) J_f(x))^\top = -\frac{d}{dt}(\nabla V_k(x))^\top = -\nabla^2 V_k(x) \dot{x}.$$

We then find that $\|\ddot{x}\| \leq \|\nabla^2 V_k(x)\| \|\dot{x}\| \leq M_k \|\dot{x}\|$. We use this bound in (9) to obtain

$$\frac{d}{dt} \frac{\|\Delta x_k\|}{\|\dot{x}\|} \leq 1 + M_k \frac{\|\Delta x_k\|}{\|\dot{x}\|}. \tag{10}$$

Now, because $\phi_k(t-t_k)$ satisfies the differential equation $\dot{\phi}_k = 1 + M_k\phi_k$ with the initial condition $\phi_k(0) = 0$, we have that $\phi_k(t-t_k) \geq \frac{\|\Delta x_k\|}{\|\dot{x}\|}$ by the Comparison Lemma, cf. [Khalil, 2002, Lemma 3.4]. Finally, we show that the bound (8) is valid for all time $[t_k, t_{k+1})$ by ruling out the possibility that $\|\dot{x}\| = 0$ along the trajectory. This can be proven by contradiction. Let $t_{\text{stop}} > t_k$ denote the first instance when $\|\dot{x}(t_{\text{stop}})\| = 0$. The resulting bound (8) is then valid for the duration $[t_k, t_{\text{stop}})$. In this duration, we note $\phi_k(t-t_k)$ is upper bounded by a positive value $\phi_k(t_{\text{stop}}-t_k)$ because it is strictly increasing. Therefore, as $\|\dot{x}(t)\| \to \|\dot{x}(t_{\text{stop}})\| = 0$, we have $\|\Delta x_k\| \to 0$. This implies $\|\Delta x_k\| = 0$ at $t = t_{\text{stop}}$, i.e., $x(t_{\text{stop}}) = x_k$. This contradicts the fact $\dot{x} \neq 0$ at $x = x_k$, concluding the proof. □

With the bound on how the state discretization error evolves given in Lemma 3.2, we next establish a lower bound on the interexecution time.

Proposition 3.3 (Lower Bound on Interexecution Time). *For the event-triggered human-robot system* (2) *with updates determined according to* (4) *and initial condition x_0, if $S_0 \subseteq \mathcal{V}$, then the interexecution time is lower bounded as*

$$t_{k+1} - t_k \geq \tau_\sigma^{\text{i}} := \frac{1}{M_0}\ln\left(1 + \frac{M_0\sigma}{L_c J_{\max}}\right) \tag{11}$$

for all $k \in \{0\} \cup \mathbb{N}$ with $J_{\max} = \max_{x\in\mathcal{S}_0}\|J_f(x)\|$.

PROOF. We aim to show that there is a finite lower bound to the time it takes before the condition defining the next update time in (4) is met. For convenience, notice that this condition can be equivalently rewritten as

$$\frac{\|\Delta x_k\|}{\|\dot{x}\|} = \frac{\sigma}{L_c\|J_f(x)\|}. \tag{12}$$

Then, by continuity, it takes longer to evolve from $\frac{\|\Delta x_k\|}{\|\dot{x}\|} = 0$ to $\frac{\|\Delta x_k\|}{\|\dot{x}\|} = \frac{\sigma}{L_c J_{\max}}$ than it takes to reach condition (12).

Now using the result (5), because $S_0 \subseteq \mathcal{V}$ we can deduce through induction that that $S_{k+1} \subset S_k \in \mathcal{V}$ for all $k \in \{0\} \cup \mathbb{N}$. From this, we note here as well that $M_k \leq M_0$ for all $k \in \{0\} \cup \mathbb{N}$. By the Comparison Lemma, we can show that $\phi_k(t-k) \leq \phi_0(t-t_k)$. Together with (8), we have $\frac{\|\Delta x_k\|}{\|\dot{x}\|} \leq \phi_0(t-t_k)$, so it takes an even shorter time for $\phi_0(t-t_k)$ to reach $\frac{\sigma}{L_c J_{\max}}$, which is precisely τ_σ^{i}. □

The lower bound on the interexecution time in Proposition 3.3 rules out the possibility of Zeno behavior. Combining this result with Proposition 3.1, we deduce asymptotic convergence towards the desired optimizer.

Corollary 3.4 (Asymptotic Stability – Ideal Human Design). *For the event-triggered human-robot system* (2) *with updates determined according to* (4)*, the optimizer x^* is asymptotically stable, with $\mathcal{X}_0 = \{x_0 \in \mathbb{R}^n \mid \mathcal{S}_0 \subseteq \mathcal{V}\}$ contained in its region of attraction. Moreover, if $c \circ f$ is strongly convex with constant $\mu > 0$ on $\mathcal{V}$, then given an initial condition $x_0 \in \mathcal{X}_0$,*

$$V(x(t)) \leq \begin{cases} V(x_k)e^{-2\mu\int_{t_k}^{t}\frac{1-\xi_0(s-t_k)}{(1+\xi_0(s-t_k))^2}ds} & , \ t \in [t_k, t_k + \tau_\sigma^{\text{i}}] \\ V(x(t_k+\tau_\sigma^{\text{i}}))e^{-\frac{2\mu(1-\sigma)}{(1+\sigma)^2}(t-t_k-\tau_\sigma^{\text{i}})} & , \ t \in [t_k+\tau_\sigma^{\text{i}}, t_{k+1}) \end{cases} \tag{13}$$

for all $k \in \{0\} \cup \mathbb{N}$, where $\xi_0(t) = L_c J_{\max}\phi_0(t)$. As a consequence, the certificate satisfies for all t,

$$V(x(t)) \leq V(x_0)e^{-\frac{2\mu(1-\sigma)}{(1+\sigma)^2}t}, \tag{14}$$

and the optimizer is exponentially stable for $\sigma \in (0,1)$.

PROOF. Asymptotic stability follows directly from Propositions 3.1 and 3.3. Next, similar to the derivation of (5) in Proposition 3.1, we can use Lemma 3.2 to bound the time derivative of the Lyapunov function as

$$\frac{d}{dt}V(x(t)) \leq -\frac{1-\xi_0(t-t_k)}{(1+\xi_0(t-t_k))^2}\|\nabla c(f(x(t)))J_f(x(t))\|^2$$

for the interval $[t_k, t_{k+1})$. Now, if $c \circ f$ is strongly convex, using (1) to bound the inequality above and also (5), we find that for $t \in [t_k, t_{k+1})$,

$$\frac{d}{dt}V(x(t)) \leq -2\mu\frac{1-\min\{\sigma, \xi_0(t-t_k)\}}{(1+\min\{\sigma, \xi_0(t-t_k)\})^2}V(x(t)).$$

To find what the min function evaluates to, we use the fact that for $t \in [t_k, t_k+\tau_\sigma^{\text{i}})$, if $t-t_k \leq \tau_\sigma^{\text{i}} = \frac{1}{M_0}\ln\left(1+\frac{M_0\sigma}{L_c J_{\max}}\right)$, then $\xi_0(t-t_k) \leq \sigma$. As a result, we separate the intervals into two accordingly to use the better bound. Using the Comparison Lemma, we get the bound (13). Finally, (14) follows by using (5) as the bound on the Lyapunov function's time derivative along the trajectory. Next, we note that from the strong convexity of function V, there exists $M \geq \mu > 0$ such that for all $x \in \mathcal{S}_0$, $\frac{\mu}{2}\|x-x^*\|^2 \leq V(x) \leq \frac{M}{2}\|x-x^*\|^2$. As a result, we deduce from (14),

$$\|x(t)-x^*\| \leq \sqrt{\frac{M}{m}}\|x_0-x^*\|e^{-\frac{\mu(1-\sigma)}{(1+\sigma)^2}t}, \tag{15}$$

and exponential stability is proven. □

Corollary 3.4 shows that one can discretize the human component of the continuous-time gradient descent of the robot motion in an opportunistic fashion while guaranteeing convergence to the desired outcome. Our results show that, under the trigger design (4), the robot can determine when to query an ideal human operator for gradient information: Proposition 3.1 states that the design choice of $\sigma \in (0,1)$ affects the magnitude of the time derivative of V, cf. (5), and therefore, the speed of convergence to the optimizer. At the same time, Proposition 3.3 suggests that σ affects the amount of trigger updates, cf. (11), and therefore the amount of human workload. The choice of σ can therefore be adjusted depending on the model of human performance, an issue that we address in the following section.

Remark 3.5 (Generalizations of Corollary 3.4). Corollary 3.4 can be generalized in a number of ways. One can, for instance, state a global version of it provided that $c \circ f$ is globally Lipschitz by taking $\mathcal{V} = \mathbb{R}^n$. This would come at the cost of having a larger constant L_c, which in turn affects the interexecution time, making it shorter, and hence increasing the human workload. Also, if the composite function $c \circ f$ is not convex, the convergence arguments employed to establish Corollary 3.4 are still valid on a sufficiently small neighborhood of a local minimizer. •

4 Event-Triggered Design: Constraints on Human Performance

In this section, we extend our trigger design and analysis to deal with practical constraints on human performance. Specifically, we consider the following models on the amount of workload that the human can take:

(1) "Need to rest" model: the human needs some time after providing gradient information before she can respond to the next query;
(2) "Need to think" model: the human cannot respond to queries instantaneously and instead requires some time to provide gradient information;
(3) "Need to think then rest" model: this is a human with both "need to rest" and "need to think" constraints.

Our treatment takes advantage of the possibility of tuning the design parameter σ to handle these constraints.

4.1 "Need To Rest" Human

We consider the scenario where the human cannot respond in quick succession to multiple queries, i.e., after providing an answer to the robot, some time must elapse before the human can respond to another query. We assume that an upper bound $T_{\text{rest}} \geq 0$ on the time the human needs for resting is known. Our first approach to this problem tunes the design parameter σ so that the interexecution time is longer than the resting time T_{rest}.

Note that, besides σ, the parameters L_c, M_0, and $J_{\max}$ also affect the bound (11) on the interexecution time. As defined, the parameters M_0 and $J_{\max}$ depend on the initial condition x_0. When dealing with the constraints on human performance, it becomes relevant to explicitly calculate the bound on the interexecution time for our design, and hence we would like them to hold independently of the initial condition $x_0 \in \mathcal{X}_0$. We assume that the set of initial conditions $\mathcal{X}_0$ satisfies $\bar{\mathcal{S}} = \{x \in \mathbb{R}^n \mid V(x) \leq \max_{x_0 \in \mathcal{X}_0} V(x_0)\} \subseteq \mathcal{V}$ (in words, the largest possible initial sublevel set of V is contained in $\mathcal{V}$). With the assumption, we can instead consider the parameters

$$\hat{M} = m \cdot \max_{x \in \mathcal{V}} \|w(x)\| \cdot \max_{x \in \mathcal{V}, i \in [m]} \|\nabla^2 f_i(x)\|,$$
$$\hat{J} = \max_{x \in \mathcal{V}} \|J_f(x)\|.$$

Note that $\hat{M} \geq M_0$ and $\hat{J} \geq J_{\max}$ for all initial conditions $x_0 \in \mathcal{X}_0$. With this in place, we define the interexecution time lower bound $\tau_\sigma^{\mathcal{V}} := \frac{1}{\hat{M}} \ln(1 + \frac{\sigma \hat{M}}{L_c \hat{J}})$, which applies to all trajectories starting in the region of attraction $\mathcal{X}_0$.

The following result shows that our trigger design of Section 3 can accommodate sufficiently small resting times.

Proposition 4.1 (Trigger for "Need to Rest" Human). *Consider the event-triggered human-robot system (2) with updates determined according to (4) and initial condition $x_0 \in \mathcal{X}_0$. If $T_{\text{rest}} < \tau_1^{\mathcal{V}} := \frac{1}{\hat{M}} \ln(1 + \frac{\hat{M}}{L_c \hat{J}})$, let $\sigma \in (0, 1]$ be such that*

$$\sigma \geq \frac{L_c \hat{J}}{\hat{M}} (e^{\hat{M} T_{\text{rest}}} - 1). \tag{16}$$

Then, $t_{k+1} \geq t_k + T_{\text{rest}}$ for all $k \in \{0\} \cup \mathbb{N}$. ∎

The proof of this result follows from Proposition 3.3 since the choice of σ satisfying (16) makes $T_{\text{rest}} \leq \tau_\sigma^{\mathcal{V}}$. If the resting time T_{rest} does not satisfy the bound identified in Proposition 4.1, then we cannot guarantee that the Lyapunov function is monotonically decreasing while the human is resting and cannot answer robot queries.

To accommodate longer resting times, we explore next the possibility of allowing the Lyapunov function to increase at times during the evolution, as long as it decreases when evaluated at consecutive human's queries (note that this corresponds to a standard discrete Lyapunov function). By doing so, we develop a new trigger design that combines both event- and time-triggered ideas. Before getting into the technical exposition, we outline here the basic rationale behind this approach, cf. Figure 1. First, we examine the

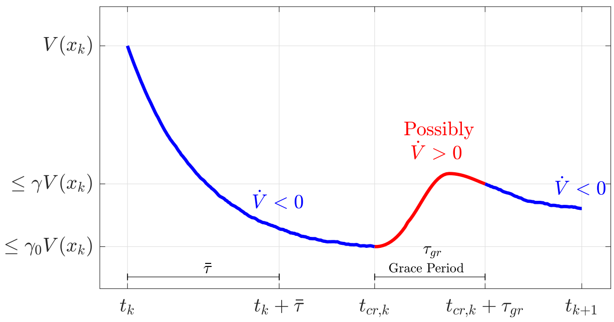

Fig. 1. Evolution of Lyapunov function with grace period. The diagram shows an example of the evolution of the Lyapunov function using our strategy to extend the resting time.

dynamics to determine a time after which the Lyapunov function V can potentially start increasing. We refer to this time as *critical.* We make the robot wait after the critical time for a pre-specified amount of time, referred to as *grace period* (later formally introduced in Proposition 4.5). This period is determined in a way that ensures that the Lyapunov function remains below its value at t_k by the end of it. After the grace period, allow the system to continue without querying the gradient information only if the Lyapunov function is decreasing.

Our first result characterizes for how long without updating the human's input and by how much we can guarantee the monotonic decrease of the Lyapunov function.

Lemma 4.2 (Trigger for Critical Time). *Consider the event-triggered human-robot system (2) and let $c \circ f$ be strongly convex with parameter μ. Define the* critical time*,*

$$t_{\text{cr},k} = \min\Big\{t \geq t_k \mid \|\Delta x_k\| = \frac{\|\nabla c(f(x_k)) J_f(x)\|}{L_c \|J_f(x)\|}\Big\}. \tag{17a}$$

If the robot does not receive any update on the gradient information from the human during $(t_k, t_{\mathrm{cr},k}]$*, then* $t_{\mathrm{cr},k} \geq t_k + \tau_1^{\mathcal{V}}$*, and*

$$V(x(t_{\mathrm{cr},k})) \leq \gamma_0 V(x_k) \tag{17b}$$

with the constant $\gamma_0 = e^{-2\mu \int_0^{\tau_1^{\mathcal{V}}} \frac{1-\xi(s)}{(1+\xi(s))^2} ds} < 1$ *and* $\xi(t) = \frac{L_c \hat{J}}{\hat{M}}(e^{\hat{M}t} - 1)$.

PROOF. Notice that the definition (17a) corresponds to (4) with $\sigma = 1$. Therefore, from (11), we deduce that $t_{\mathrm{cr},k} - t_k \geq \tau_1^{\mathrm{i}} \geq \tau_1^{\mathcal{V}}$. If the robot does not receive any update on the gradient information from the human during $(t_k, t_{\mathrm{cr},k}]$, then, using (13), we deduce that

$$V(x(t)) \leq \begin{cases} V(x_k) e^{-2\mu \int_{t_k}^{t} \frac{1-\xi(s-t_k)}{(1+\xi(s-t_k))^2} ds} & \text{if } t \in [t_k, t_k + \tau_1^{\mathcal{V}}], \\ V(x(t_k + \tau_1^{\mathcal{V}})) & \text{if } t \in [t_k + \tau_1^{\mathcal{V}}, t_{\mathrm{cr},k}), \end{cases}$$

which implies (17b). $\square$

The expression (17b) estimates how much the Lyapunov function has decreased before we can no longer guarantee that it will not increase. Next, we turn our attention to bound how much the Lyapunov may increase after the critical time if the robot does not get updated gradient information from the human. To find such a bound, we make the following additional assumption.

Assumption 4.3 (Strong Convexity of the Composition Function). The composition function $c \circ f$ is strongly convex with parameter μ as a consequence of

(1) each objective function $f_i \in \{f_i\}_{i \in [m]}$ being strongly convex; and
(2) the cost function c being strictly convex and increasing with respect to each component. •

Under Assumption 4.3, the function $V_k(x) = w(x_k)f(x)$ is strongly convex because every component of w is always positive. Therefore, there exist a strongly convex parameter $\mu_k > 0$ such that $\mu_k I \preceq \nabla^2 V_k(x)$. Define also

$$\hat{\mu} = \min_{x \in \mathcal{V}} \|w(x)\| \cdot \min_{x \in \mathcal{V}, i \in [m]} \|\nabla^2 f_i(x)\|,$$

and note that, by definition, $\hat{\mu} \leq \mu_k$ for all k. Our next result characterizes how fast the Lyapunov function increases after the critical time, and how long it will take for the function to exceed the amount it previously decreased.

Lemma 4.4 (Lyapunov Function Bound After Critical Time). *Consider the event-triggered human-robot system* (2) *with Assumption 4.3. If* t_{k+1} *is such that* $x(t) \in S_k$*, for all* $t \in [t_k, t_{k+1})$*, and* $t_{k+1} \geq t_{\mathrm{cr},k}$*, then*

$$V(x(t)) \leq V(x(t_{\mathrm{cr},k})) + V(x(t_k))\beta(t) \tag{18a}$$

for $t \in [t_{\mathrm{cr},k}, t_{k+1}]$*, where* β *is the strictly increasing function*

$$\beta(t) = \frac{2\hat{M}^2}{\hat{\mu}} \int_{t_{\mathrm{cr},k}}^{t} (\xi(s - t_{\mathrm{cr},k} + \tau_1^{\mathcal{V}}) - 1) e^{-2\hat{\mu}(s-t_k)} ds. \tag{18b}$$

with $\xi(t) = \frac{L_c \hat{J}}{\hat{M}}(e^{\hat{M}t} - 1)$.

PROOF. We begin by finding a bound on the state deviation after the critical time. The assumption on t_{k+1} is the same as that of Lemma 3.2, so we can deduce (10). Because $\hat{M} \geq M_k$, we can find

$$\frac{d}{dt} \frac{\|\Delta x_k\|}{\|\dot{x}\|} \leq 1 + \hat{M} \frac{\|\Delta x_k\|}{\|\dot{x}\|}$$

for $t \in [t_k, t_{k+1})$. From (17a), we note that $\frac{\|\Delta x_k\|}{\|\dot{x}\|} \leq \frac{1}{L_c \hat{J}}$ at time $t_{\mathrm{cr},k}$. Using the Comparison Lemma with dynamics $\dot{\phi} = 1 + \hat{M}\phi$ and initial condition $\phi(t_{\mathrm{cr},k}) = \frac{1}{L_c \hat{J}}$, we have

$$\begin{aligned} \frac{\|\Delta x_k\|}{\|\dot{x}\|} &\leq \frac{1}{\hat{M}} \left(\Big(1 + \frac{\hat{M}}{L_c \hat{J}}\Big) e^{\hat{M}(t - t_{\mathrm{cr},k})} - 1 \right) \\ &\leq \frac{1}{\hat{M}} (e^{\hat{M}(t - t_{\mathrm{cr},k} + \tau_1^{\mathcal{V}})} - 1) \end{aligned}$$

for $t \in [t_{\mathrm{cr},k}, t_{k+1})$. We use this bound in the time derivative of the Lyapunov function along the trajectory as follows,

$$\begin{aligned} \frac{d}{dt} V(x(t)) &\leq -\|w(x_k)J_f(x)\|^2 + \|\Delta w_k J_f(x)\| \|w(x_k)J_f(x)\| \\ &\leq -\|w(x_k)J_f(x)\|^2 \\ &\quad + L_c \|\Delta x_k\| \|J_f(x)\| \|w(x_k)J_f(x)\| \\ &\leq -\|w(x_k)J_f(x)\|^2 + L_c \hat{J} \frac{\|\Delta x_k\|}{\|\dot{x}\|} \|w(x_k)J_f(x)\|^2 \\ &\leq (-1 + \xi(t - t_{\mathrm{cr},k} + \tau_1^{\mathcal{V}})) \|w(x_k)J_f(x)\|^2. \end{aligned} \tag{19}$$

for $t \in [t_{\mathrm{cr},k}, t_{k+1})$. By definition, $\xi(t)$ is strictly increasing and $\xi(\bar{\tau}) = 1$, therefore $\xi(t - t_{\mathrm{cr},k} + \tau_1^{\mathcal{V}}) - 1 > 0$ for $t > t_{\mathrm{cr},k}$. Therefore, we proceed by finding the upper bound to $\|w(x_k)J_f(x(t))\|^2$ using (1) as follows

$$\begin{aligned} \|w(x_k)J_f(x(t))\|^2 &\leq 2\hat{M} V_k(x(t)) \overset{(a)}{\leq} 2\hat{M} e^{-2\hat{\mu}(t-t_k)} V_k(x_k) \\ &\leq \frac{\hat{M}}{\hat{\mu}} e^{-2\hat{\mu}(t-t_k)} \|w(x_k)J_f(x_k)\|^2 \\ &\leq \frac{2\hat{M}^2}{\hat{\mu}} e^{-2\hat{\mu}(t-t_k)} V(x_k), \end{aligned}$$

where (a) follows from $\frac{d}{dt} V_k(x(t)) = -\|w(x_k)J_f(x(t))\|^2 \leq -2\hat{\mu} V_k(x(t))$. Substituting in (19), we obtain

$$\frac{d}{dt} V(x(t)) \leq (\xi(t - t_{\mathrm{cr},k} + \tau_1^{\mathcal{V}}) - 1) \Big(\frac{2\hat{M}^2}{\hat{\mu}} e^{-2\hat{\mu}(t-t_k)} V(x_k) \Big),$$

and the result follows via the Comparison Lemma. $\square$

The combination of Lemmas 4.2 and 4.4 bounds the evolution of the Lyapunov function before and after the critical time. With these results, we can use guarantee an overall decrease between two interexecution times despite some increase in the Lyapunov function after the critical time. Using this idea, we propose a novel event-triggered design.

Proposition 4.5 (Trigger for "Need to Rest" Human using Grace Period). *Consider the human-robot* *system* (2) *with Assumption 4.3. For* $\gamma \in [\gamma_0, 1)$, *let the* grace period $\tau_{\rm gr}$ *be the solution to*

$$\gamma - \gamma_0 = \frac{2\hat{M}^2}{\hat{\mu}} \int_{\tau_1^{\mathcal{V}}}^{\tau_{\rm gr}+\tau_1^{\mathcal{V}}} (\xi(s) - 1)e^{-2\hat{\mu}s} ds.$$

For $T_{\rm rest} \in [\tau_1^{\mathcal{V}}, \tau_{\rm gr} + \tau_1^{\mathcal{V}}]$, *let the updates* $\{t_{k+1}\}_{k\in\{0\}\cup\mathbb{N}}$ *be determined according to*

$$t_{k+1} = \min\Big\{t \geq t_{{\rm cr},k}+\tau_{\rm gr} \mid \|\Delta x_k\| \geq \frac{\|\nabla c(f(x_k))J_f(x)\|}{L_c\|J_f(x)\|}\Big\}. \tag{20}$$

Then, for each $k \in \{0\} \cup \mathbb{N}$, $V(x(t_{k+1})) \leq \gamma V(x(t_k))$, *and* $t_{k+1} - t_k \geq T_{\rm rest}$. *As a result, the optimizer is asymptotically stable, with* $\mathcal{X}_0$ *contained in its region of attraction, and*

$$V(x(t_k)) \leq \gamma^k V(x_0). \tag{21}$$

PROOF. Note that due to the trigger design (20), $t_{k+1} \geq t_{{\rm cr},k}$, and therefore, both Lemma 4.2 and Lemma 4.4 hold. We use the following bounds

$$\begin{aligned}
&\beta(t_{{\rm cr},k} + \tau_{\rm gr}) \\
&= \frac{2\hat{M}^2}{\hat{\mu}} \int_{t_{{\rm cr},k}}^{t_{{\rm cr},k}+\tau_{\rm gr}} (\xi(s - t_{{\rm cr},k} + \tau_1^{\mathcal{V}}) - 1)e^{-2\hat{\mu}(s-t_k)} ds \\
&= \frac{2\hat{M}^2}{\hat{\mu}} \int_{\tau_1^{\mathcal{V}}}^{\tau_{\rm gr}+\tau_1^{\mathcal{V}}} (\xi(s) - 1)e^{-2\hat{\mu}(s-t_k+t_{{\rm cr},k}-\tau_1^{\mathcal{V}})} ds \\
&\leq \frac{2\hat{M}^2}{\hat{\mu}} \int_{\tau_1^{\mathcal{V}}}^{\tau_{\rm gr}+\tau_1^{\mathcal{V}}} (\xi(s) - 1)e^{-2\hat{\mu}s} ds = \gamma - \gamma_0
\end{aligned}$$

where the inequality holds because $\xi(s) - 1 \geq 0$ for $s \geq \tau_1^{\mathcal{V}}$, and $t_k - t_{{\rm cr},k} + \bar{\tau} \leq 0$ from Lemma 4.2. Substituting the inequality above and (17b) to evaluate (18a), we obtain

$$\begin{aligned}
V(x(t_{{\rm cr},k} + \tau_{\rm gr} - \tau_1^{\mathcal{V}})) &\leq \gamma_0 V(x_k) + (\gamma - \gamma_0)V(x_k) \\
&= \gamma V(x_k).
\end{aligned}$$

Now, for $t \in [t_{{\rm cr},k} + \tau_{\rm gr} - \tau_1^{\mathcal{V}}, t_{k+1})$, we can find that $\|\Delta x_k\| < \sigma\Big(\frac{\|\nabla c(f(x_k))J_f(x)\|}{L_c\|J_f(x)\|}\Big)$. As such, (6) holds and Lyapunov function decreases during the duration. In other words, $V(x(t_{k+1})) \leq \gamma V(x_k)$, and (21) follows. Finally, because $t_{{\rm cr},k} - \tau_1^{\mathcal{V}} \geq t_k$, we note that $t_{k+1} \geq t_k + \tau_{\rm gr} + \tau_1^{\mathcal{V}}$ by design, so $t_{k+1} - t_k \geq T_{\rm rest}$ as claimed. Since the design is Zeno-free, the optimizer is asymptotically stable. □

Note that the grace period $\tau_{\rm gr}$ can be determined offline given the various problem parameters and the design parameter γ. Proposition 4.5 offers a strategy for accommodating longer resting times than the ones obtained in Proposition 4.1. Let us recapture here the ideas behind the trigger design (20) that allows to accomplish this. After each human update, we use the trigger (17a) to determine $t_{{\rm cr},k}$, where we know the decrease in V given by (17b). We then let the system proceed without any human update for $\tau_{\rm gr}$. In this period, the definition of $\tau_{\rm gr}$ in Proposition 4.5 guarantees that V can increase but cannot exceed $\gamma V(x_k)$, which is a direct result from Lemma 4.4. Finally, we let the system continue with trigger (20), which will prescribe an update once V stops decreasing (this might be immediate). As a consequence, our design ensures that the Lyapunov function decreases between two consecutive execution times.

The design parameter γ directly corresponds to the convergence rate guarantee, cf. (21). Note that the convergence rate is given with respect to the number of iterations rather than time, which are not equivalent when the interexecution time is not fixed. In any case, much like how the accommodation of longer resting times increases the value σ in Proposition 4.1, here it requires a larger value of γ, which slows down the convergence rate.

4.2 "Need to Think" Human

In this section, we deal with the case when the human does not respond instantaneously to queries from the robot and instead, once asked, takes some time "to think" and provide information. Formally, for each $k \in \{0\}\cup\mathbb{N}$, when the robot asks the human at time t_{k+1} for the evaluation of the gradient ∇c at $f(x_{k+1})$, the human takes some time $D_{k+1} \geq 0$ to relay the information $\nabla c \circ f(x_{k+1})$. This means that, up until $t_{k+1} + D_{k+1}$, the robot still uses the "old" information $\nabla c \circ f(x_k)$ provided in the previous communication with the human. The dynamics is then given by

$$\dot{x} = -(\nabla c(f(x_k))J_f(x))^\top, \tag{22}$$

for $t \in [t_k + D_k, t_{k+1} + D_{k+1}]$. Human thinking time spans are not necessarily equal across different time instants, but we assume them to be uniformly upper bounded by a known constant $T_{\rm thk} > 0$, representing the maximum time it takes the human to relay her gradient information. Regarding the initialization of the dynamics, we assume that the optimization starts when the human gives his initial gradient information, and therefore, $D_0 = 0$.

Given the model above, there are two new complications that arise in designing the event-triggered law. First, it is clear that the robot should not wait until it absolutely needs the new gradient information available to request it from the human, as it did in the ideal human case considered in Section 3. In other words, if we were to define the time at which the trajectory satisfies the condition for (4) as

$$t_{{\rm nec},k} = \min\Big\{t \geq t_k \mid \|\Delta x_k\| = \frac{\sigma\|\nabla c(f(x_k))J_f(x(t))\|}{L_c\|J_f(x(t))\|}\Big\},$$

then we would like $t_{k+1} + D_{k+1}$ to occur before $t_{{\rm nec},k}$ to ensure condition (5), like we did in the ideal human case. However, this is not simple as subtracting $T_{\rm thk}$ from $t_{{\rm nec},k}$ because we do not know exactly what $t_{{\rm nec},k}$ is since it is determined by an event. The robot should anticipate the human delay in responding and ask in advance, ideally D_{k+1} before the need for updated information arises. Another complication in designing a trigger is that the trigger may occur too often. We assume that when queried, the human operator is busy during the time interval $[t_{k+1}, t_{k+1} + D_{k+1}]$, and therefore cannot accept another query during this time.

In summary, we want our new design to prescribe t_{k+1} satisfying the following:

- t_{k+1} occurs before $t_{{\rm nec},k} - D_{k+1}$;
- t_{k+2} happens after $t_{k+1} + D_{k+1}$ when prescribed iteratively.

To achieve these objectives, we use a similar trigger design as in the ideal human case with a new design parameter σ'. Our strategy is based on tuning this parameter so that t_{k+1} neither occurs too late nor too early. This is done by estimating how long after t_{k+1} it takes for $t_{\mathrm{nec},k}$ to occur, and how long it takes for t_{k+2} to occur after t_{k+1}. The following result makes this statement precise.

Proposition 4.6 (Trigger for "Need to Think" Human). *Consider the event-triggered human-robot system* (22). *With* $\sigma \in (0,1)$, *let* D^*_{thk} *be the unique solution to*

$$\left(\frac{1+\sigma}{1-\sigma}\right)^2 = \frac{e^{\hat{M}(\tau^{\mathcal{V}}_\sigma - D^*_{\mathrm{thk}})} - 1}{e^{\hat{M}D^*_{\mathrm{thk}}} - 1},$$

and assume $D^*_{\mathrm{thk}} > T_{\mathrm{thk}}$. *Let* $\sigma' \in (0,1)$ *be such that*

$$\frac{L_c\hat{J}}{\hat{M}}\left(\frac{1+\sigma}{1-\sigma}\right)^2 (e^{\hat{M}T_{\mathrm{thk}}} - 1) < \sigma' \le \frac{L_c\hat{J}}{\hat{M}}(e^{\hat{M}(\tau^{\mathcal{V}}_\sigma - T_{\mathrm{thk}})} - 1). \tag{23}$$

For $k \in \{0\} \cup \mathbb{N}$, *let* t_{k+1} *be determined by*

$$t_{k+1} = \min\left\{t \ge t_k \mid \|\Delta x_k\| = \frac{\sigma'\|\nabla c(f(x_k))J_f(x)\|}{L_c\hat{J}}\right\}. \tag{24}$$

Then, for each $k \in \{0\}\cup\mathbb{N}$, *we have* $\|\Delta x_k\| < \frac{\sigma\|\nabla c(f(x_k))J_f(x)\|}{L_c\|J_f(x)\|}$ *for* $t \in [t_k, t_{k+1} + D_{k+1})$, $t_{k+2} > t_{k+1} + D_{k+1}$, *and as a consequence, the performance guarantee* (5) *on the Lyapunov function holds for all* $t \in [t_k + D_k, t_{k+1} + D_{k+1})$.

PROOF. We start by guaranteeing the existence of σ'. For this, we simply show that the upper bound in (23) is greater than or equal to the lower bound, or equivalently,

$$\left(\frac{1+\sigma}{1-\sigma}\right)^2 < \frac{e^{\hat{M}(\tau^{\mathrm{i}}_\sigma - T_{\mathrm{thk}})} - 1}{e^{\hat{M}T_{\mathrm{thk}}} - 1}$$

The right hand side is strictly decreasing with respect to T_{thk}. Given the definition of D^*_{thk}, we deduce that all $T_{\mathrm{thk}} < D^*_{\mathrm{thk}}$ satisfy the inequality. Note also that $\sigma' \le \sigma$.

Next, with a slight abuse of notation, we use $\dot{x}^{[k]} = (\nabla c(f(x_k))J_f(x))^\top$. We resort to Table 1 to help specify desired values of $\|\Delta x\|$ in effect at different time intervals.

Table 1
Desired state deviation at different time intervals.

Interval	$(t_k + D_k, t_{k+1})$	t_{k+1}	$(t_{k+1}, t_{k+1} + D_{k+1})$
$\|\Delta x_k\|$	$< \frac{\sigma'\|\dot{x}^{[k]}\|}{L_c\hat{J}}$	$\frac{\sigma'\|\dot{x}^{[k]}\|}{L_c\hat{J}}$	$< \frac{\sigma\|\dot{x}^{[k]}\|}{L_c\|J_f(x)\|}$
$\|\Delta x_{k+1}\|$	Undefined	0	$< \frac{\sigma'\|\dot{x}^{[k+1]}\|}{L_c\hat{J}}$

The first part of the proof focuses on the evolution of $\|\Delta x_k\|$. As shown in the last column of Table 1, the trigger (24) requesting the gradient at time t_{k+1} should not violate $\|\Delta x_k\| < \sigma\left(\frac{\|\dot{x}^{[k]}\|}{L_c\|J_f(x)\|}\right)$ up until the gradient implementation at $t_{k+1} + D_{k+1}$. To do so, we would like D_{k+1} to be shorter than the time it takes for $\frac{\|\Delta x_k\|}{\|\dot{x}^{[k]}\|}$ to evolve, from $\frac{\sigma'}{L_c\hat{J}}$ to $\frac{\sigma}{L_c\hat{J}}$ (Notice that $\frac{\sigma}{L_c\hat{J}} < \frac{\sigma}{L_c\|J_f(x)\|}$, $\forall x \in \mathcal{X}_0$). This leads to applying the Comparison Lemma with the function ϕ satisfying $\dot{\phi} = 1 + \hat{M}\phi$ with $\phi(t_{k+1}) = \frac{\sigma'}{L_c\hat{J}}$, and asking for

$$D_{k+1} \le \frac{1}{\hat{M}}\ln(1 + \hat{M}\frac{\sigma}{L_c\hat{J}}) - \frac{1}{\hat{M}}\ln(1 + \hat{M}\frac{\sigma'}{L_c\hat{J}}).$$

To ensure this condition, we can select σ' so that the right hand side is an upper bound on T_{thk}, which leads to the upper bound on σ' in (23).

The second part of the proof examines the possibility of the state error $\|\Delta x_{k+1}\|$ to begin with a larger value than the trigger value at the time $t_{k+1} + D_{k+1}$ of implementation of the new gradient. This is possible because Δx_{k+1} evolves with $\dot{x}^{[k]}$ until $t_{k+1} + D_{k+1}$. For this, let $T_{\mathrm{allow}} = t_{k+2} - t_{k+1}$ be the time it takes $\|\Delta x_{k+1}\|$ to evolve from 0 to $\frac{\sigma'\|\dot{x}^{[k+1]}\|}{L_c\hat{J}}$ with the dynamics $\dot{x} = \dot{x}^{[k]}$. We will show that enforcing the lower bound on σ' in (23) ensures $D_{k+1} \le T_{\mathrm{allow}}$. We reason by contradiction. Assume $D_{k+1} > T_{\mathrm{allow}}$ and let us examine the dynamics of $\frac{\|\Delta x_{k+1}\|}{\|\dot{x}^{[k]}\|}$. Following a similar derivation as in the proof of Lemma 3.2, we arrive at

$$\frac{d}{dt}\frac{\|\Delta x_{k+1}\|}{\|\dot{x}^{[k]}\|} \le \frac{\|\dot{x}^{[k+1]}\|}{\|\dot{x}^{[k]}\|} + \hat{M}\frac{\|\Delta x_{k+1}\|}{\|\dot{x}^{[k]}\|}. \tag{25}$$

We next proceed to bound $\frac{\|\dot{x}^{[k+1]}\|}{\|\dot{x}^{[k]}\|}$. Note that, from (7), we have $\|w(x)J_f(x)\| \le (1+\sigma)\|\dot{x}^{[k]}\|$ for $t \in [t_k, t_{k+1} + D_{k+1}]$. Additionally, from $w(x_k)J_f(x) = (w(x) - \Delta w_k)J_f(x)$,

$$\begin{aligned}\|w(x_{k+1})J_f(x)\| &\le \|w(x)J_f(x)\| + \|\Delta w_{k+1}\|\|J_f(x)\| \\ &\le \|w(x)J_f(x)\| + L_c\|\Delta x_{k+1}\|\|J_f(x)\| \\ &\le \|w(x)J_f(x)\| + \sigma'\|w(x_{k+1})J_f(x)\| \\ &\le \|w(x)J_f(x)\| + \sigma\|w(x_{k+1})J_f(x)\|,\end{aligned}$$

during $t \in [t_{k+1}, t_{k+1} + T_{\mathrm{allow}}]$. Using this in conjunction with (7) and the fact that $T_{\mathrm{allow}} < D_{k+1}$, we have

$$(1-\sigma)\|\dot{x}^{[k+1]}\| \le \|w(x)J_f(x)\| \le (1+\sigma)\|\dot{x}^{[k]}\|,$$

valid for $t \in [t_{k+1}, t_{k+1} + T_{\mathrm{allow}}]$, and hence $\frac{\|\dot{x}^{[k+1]}\|}{\|\dot{x}^{[k]}\|} \le \frac{1+\sigma}{1-\sigma}$. Substituting this ratio in (25), we get

$$\frac{d}{dt}\frac{\|\Delta x_{k+1}\|}{\|\dot{x}^{[k]}\|} \le \frac{1+\sigma}{1-\sigma} + \hat{M}\frac{\|\Delta x_{k+1}\|}{\|\dot{x}^{[k]}\|}.$$

Now, we solve for $\dot{\psi} = \frac{1+\sigma}{1-\sigma} + \hat{M}\psi$ with initial condition $\psi(t_{k+1}) = 0$, and use the Comparison Lemma to ensure

$$\psi(t_{k+1} + T_{\mathrm{allow}}) = \frac{(1+\sigma)}{\hat{M}(1-\sigma)}(e^{\hat{M}T_{\mathrm{allow}}} - 1) \ge \frac{\|\Delta x_{k+1}\|}{\|\dot{x}^{[k]}\|}.$$

Recall this inequality is true for all $t \in [t_{k+1}, t_{k+1} + T_{\mathrm{allow}}]$ where we can use once again the relationship $\|\dot{x}^{[k+1]}\| \ge \frac{1-\sigma}{1+\sigma}\|\dot{x}^{[k]}\|$. Therefore, at $t = t_{k+1} + T_{\mathrm{allow}}$,

$$\frac{\sigma'}{L_c\hat{J}} = \frac{\|\Delta x_{k+1}\|}{\|\dot{x}^{[k+1]}\|} \le \frac{1}{\hat{M}}\left(\frac{1+\sigma}{1-\sigma}\right)^2 (e^{\hat{M}T_{\mathrm{allow}}} - 1) \tag{26}$$

Using now the lower bound in (23), we deduce $T_{\text{thk}} < T_{\text{allow}}$, which is a contradiction because $T_{\text{thk}} > D_{k+1}$. Therefore, $D_{k+1} \le T_{\text{allow}}$. Since $t_{k+2} = t_{k+1} + T_{\text{allow}}$, we have $t_{k+2} > t_{k+1} + D_{k+1}$. Finally, since at all times $t \in [t_k + D_k, t_{k+1} + D_{k+1})$, we have bounded $\|\Delta x_k\| \le \sigma \left(\frac{\|\nabla(c(f(x_k)))J_f(x)\|}{L_c \|J_f(x)\|} \right)$, the Lyapunov function rate (5) is ensured. □

Proposition 4.6 requires the thinking time T_{thk} to be smaller than D^*_{thk}. Consistent with the treatment of delays in the event-triggered control literature [Dolk et al., 2017, Hetel et al., 2006, Li et al., 2012, Wu et al., 2015], it does not come as a surprise that the thinking time must be sufficiently small for a trigger design to exist; otherwise, the system will receive no human updates for too long and start behaving unsatisfactorily. D^*_{thk} can then be interpreted as the maximum allowable thinking time for the human. Although we interpret the delays as caused by the human's thinking time, other sources of delay could be equally accommodated by Proposition 4.6.

Similarly to the ideal human case of Section 3, to ensure convergence, we need to show that the trigger (24) will not exhibit Zeno behavior. The following result provides a uniform lower bound on the interexecution time.

Proposition 4.7 (Interexecution Time with Update Delay). *For the event-triggered human-robot system* (22) *with updates determined according to* (24)*, and under the same hypotheses as Proposition 4.6, the interexecution time is lower bounded as* $t_{k+1} - t_k \ge \tau^{\text{thk}}_{\sigma'}$ *where*

$$\tau^{\text{thk}}_{\sigma'} := \frac{1}{\hat{M}} \ln \left(\frac{1 + \hat{M} \frac{\sigma'}{L_c J_{\max}}}{1 + \left(\frac{1+\sigma}{1-\sigma}\right)^2 (e^{\hat{M} T_{\text{thk}}} - 1)} \right) + T_{\text{thk}}. \quad (27)$$

PROOF. By construction, during $[t_k + D_k, t_{k+1}]$, the dynamics is given by $\dot{x}^{[k]}$. Similarly to how we obtained inequality (26) in the proof of Proposition 4.6, we have

$$\frac{\|\Delta x_k\|}{\|\dot{x}^{[k]}\|} \le \frac{1}{\hat{M}} \left(\frac{1+\sigma}{1-\sigma} \right)^2 (e^{\hat{M} D_k} - 1),$$

at time $t_k + D_k$. Setting $\phi(t_k + D_k)$ equal to the right hand side of the above inequality as the initial condition, we solve the dynamics $\dot{\phi} = 1 + \hat{M}\phi$,

$$\frac{1}{\hat{M}} \ln \left(\frac{1 + \hat{M}\phi(t)}{1 + \hat{M}\phi(t_k + D_k)} \right) = t - (t_k + D_k),$$

for $t \ge t_k + D_k$. Using the Comparison Lemma, we know $\frac{\|\Delta x_k\|}{\|\dot{x}^{[k]}\|} \le \phi(t)$, so it takes longer time for $\frac{\|\Delta x_k\|}{\|\dot{x}^{[k]}\|}$ to evolve to $\frac{\sigma'}{L_c \hat{J}}$ (precisely $t_{k+1} - t_k - D_k$) than it takes $\phi(t_k + D_k)$ to increase to $\phi(t) = \frac{\sigma'}{L_c \hat{J}}$. As such, we find that

$$t_{k+1} - t_k \ge \frac{1}{\hat{M}} \ln \left(\frac{1 + \hat{M} \frac{\sigma'}{L_c J_{\max}}}{1 + \left(\frac{1+\sigma}{1-\sigma}\right)^2 (e^{\hat{M} D_k} - 1)} \right) + D_k.$$

The result now follows by observing that the right hand side is decreasing in D_k. □

The combination of Propositions 4.6 and 4.7 ensures that the event-triggered human-robot system (22) with updates determined according to (24) enjoys the same convergence guarantee as stated in Corollary 3.4.

Corollary 4.8 (Asymptotic Stability – "Need to Think" Human Design). *For the event-triggered human-robot system* (22) *with updates determined according to* (24)*, the optimizer* x^* *is asymptotically stable, with* $\mathcal{X}_0 = \{x_0 \in \mathbb{R}^n \mid \mathcal{S}_0 \subseteq \mathcal{V}\}$ *contained in its region of attraction. Moreover, if* $c \circ f$ *is strongly convex with constant* $\mu > 0$ *on* $\mathcal{V}$*, then given an initial condition* $x_0 \in \mathcal{X}_0$*,* (13) *holds for all* $k \in \{0\} \cup \mathbb{N}$*. As a consequence, the optimizer is exponentially stable with the bound* (14) *for* $\sigma \in (0, 1)$*.* □

4.3 "Need to Think Then Rest" Human

Here, we combine the "need to rest" and "need to think" models into a single one: not only does the human take some time in responding to a robot's query, but she also has to rest before she can reply to the robot again. Formally, this means that the robot follows the dynamics (22) with the additional constraint that $t_{k+1} \ge t_k + D_k + T_{\text{rest}}$ for all $k \in \{0\} \cup \mathbb{N}$. Our next result addresses this problem.

Proposition 4.9 (Trigger for "Need to Think Then Rest" Human). *Consider the event-triggered human-robot system* (22)*. Given* $\sigma \in (0, 1)$ *and* T_{rest}*, let* $D^*_{\text{tnk-rst}}$ *be the unique solution to*

$$\left(\frac{1+\sigma}{1-\sigma} \right)^2 = \frac{e^{\hat{M}(\tau^{\mathcal{V}}_{\sigma} - D^*_{\text{tnk-rst}} - T_{\text{rest}})} - 1}{e^{\hat{M} D^*_{\text{tnk-rst}}} - 1}, \quad (28)$$

and assume $D^*_{\text{tnk-rst}} > T_{\text{thk}}$*. For* $k \in \{0\} \cup \mathbb{N}$*, let* t_{k+1} *be determined according to* (24)*, where* $\sigma' \in (0, 1)$ *is such that*

$$\frac{L_c \hat{J}}{\hat{M}} \Big(\left(\frac{1+\sigma}{1-\sigma} \right)^2 (e^{\hat{M} T_{\text{thk}}} - 1) e^{\hat{M} T_{\text{rest}}} + (e^{\hat{M} T_{\text{rest}}} - 1) \Big) < \sigma' \le \frac{L_c \hat{J}}{\hat{M}} (e^{\hat{M}(\tau^{\mathcal{V}}_{\sigma} - T_{\text{thk}})} - 1).$$

Then, for each $k \in \{0\} \cup \mathbb{N}$*, we have* $\|\Delta x_k\| < \frac{\sigma \|\nabla c(f(x_k)) J_f(x)\|}{L_c \|J_f(x)\|}$ *for* $t \in [t_k, t_{k+1} + D_{k+1})$*,* $t_{k+2} > t_{k+1} + D_{k+1} + T_{\text{rest}}$*, and as a consequence, the bound* (5) *on the evolution of the Lyapunov function holds for all time,* $t \in [t_k + D_k, t_{k+1} + D_{k+1})$*.*

PROOF. First, note that the newly introduced rest time constraint has no effect on how the upper bound is derived in (23), so it remains the same here. On the other hand, the lower bound to σ' is affected by the rest time constraint. Specifically, we must now guarantee that the value of $\|\Delta x_{k+1}\|$ must not exceed the trigger condition $\frac{\sigma' \|\dot{x}^{[k+1]}\|}{L_c J_{\max}}$, but at the time $t_{k+1} + D_{k+1} + T_{\text{rest}}$ (instead of the earlier $t_{k+1} + D_{k+1}$). We break the time of interest into two intervals, $[t_{k+1}, t_{k+1} + D_{k+1}]$ and $[t_{k+1} + D_{k+1}, t_{k+1} + D_{k+1} + T_{\text{rest}}]$ because in these two intervals, the dynamics are different due to the human's update.

First, we focus on the latter of the two time intervals. From (9),

$$\frac{d}{dt} \frac{\|\Delta x_{k+1}\|}{\dot{x}^{[k+1]}} \le 1 + \hat{M} \frac{\|\Delta x_{k+1}\|}{\dot{x}^{[k+1]}}.$$

As such, we know that if

$$\frac{\|\Delta x_{k+1}\|}{\dot{x}^{[k+1]}} \leq \frac{1}{\hat{M}}\left((1+\hat{M}\frac{\sigma'}{L_c J_{\max}})e^{-\hat{M}T_{\text{rest}}}-1\right),$$

at time $t_{k+1}+D_{k+1}$, then $\frac{\|\Delta x_{k+1}\|}{\dot{x}^{[k+1]}} \leq \frac{\sigma'}{L_c J_{\max}}$ at time $t_{k+1}+D_{k+1}+T_{\text{rest}}$ by using the Comparison Lemma. Next, we deal with the interval $[t_{k+1}, t_{k+1}+D_{k+1}]$ to show that the lower bound given in the statement ensures the above inequality at time $t_{k+1}+D_{k+1}$. This can be done by following the same contradiction proof procedure as presented for Proposition 4.6. □

Proposition 4.9 gives a method to deal with both human resting and thinking time. Once again, these constraints must be sufficiently small. We can interpret $D^*_{\text{thk-rst}}$ as the maximum allowable thinking time for the human, given the amount of time he needs to rest. As Zeno behavior is absent due to the interexecution time being lower bounded by the resting time, an analogous statement to Corollary 4.8 follows. The given model is the richest in term of dealing with constraints on human performance, and we can recover earlier models by setting resting or thinking time to zero.

Remark 4.10 (Units of Time). The two types of constraints on human performance considered here both have parameters dealing with time. The resting time T_{rest} and the thinking time D most likely will be quantified with units of time that are meaningful in the real world (e.g., seconds and hours). On the other hand, the gradient descent has its own unit of time that is encoded in the dynamics. To use our results, it is important to reconcile the difference in units. One way to do this is by noting that the gradient descent is calculated by the robot. In practice, the robot will probably implement the continuous gradient dynamics through a discretization with a constant stepsize. Given how long the robot takes to compute each step in the gradient descent, we have a convenient unit conversion between the two time units. We note here that the conversion depends on the robot's computing power and the selected stepsize. •

5 Simulations

We consider a human-robot interaction scenario where a human aids the robot in determining a safe trajectory through an environment populated with threats of different levels. The robot is tasked to travel from the origin at $(0,0)$ to $(1,0)$ on the xy-plane. The robot has scanned a few potential threats in the area with positions among

$$(x_{\text{obs}}, y_{\text{obs}}) = \{(0.8, 0.1),\ (0.3, -0.2),\ (0.2, 0.04),\\ (0.68, 0.3),\ (0.5, 0.12)\}.$$

Ideally, the robot would like to stay away from these locations while, at the same time, would like to traverse the shortest path possible to its goal. To describe its reference trajectory, the robot uses a sum of sinusoidal functions as,

$$y = \sum_{i=1}^{10} a_i \sin(i\pi x),\ x \in [0,1],$$

where $a \in \mathbb{R}^{10}$ are the amplitudes to be optimized. The objective functions for avoiding obstacles and for measuring path length are given by

$$f_{\text{obs},j}(a) = -\max_{x\in[0,1]}\left\{(y_{\text{obs},j}-y)^2+(x_{\text{obs},j}-x)^2\right\},$$

$$f_{\text{len}}(a) = \int_0^1 \sqrt{1-(\sum_{i=1}^{10} i\pi a_i\cos(i\pi x))^2}\,dx,$$

for $j \in [5]$ and $a \in \mathbb{R}^{10}$. In order to find the amplitudes that best describe the most desired reference trajectory, a human works with the robot in the multiobjective optimization problem with objective functions $f_{\text{obs},1}, \dots, f_{\text{obs},5}, f_{\text{len}}$ by evaluating risks of the likely threats and providing the robot with gradient information. In practice, the human preference function is not known, and the gradient information can only be estimated, perhaps through asking the human to rate the importance of each objective functions at a given point. For the purpose of the simulation, we use the following function to represent the human preferences,

$$c(f) = \frac{f_{\text{len}}^2}{10} + \sum_{j=1}^{5} \frac{q_j}{f_{\text{obs},j}^2},$$

where $q = [0.2, 0.5, 0.03, 0.1, 0.3]$. The weights captured in q represent how the human assesses the threats. The third potential threat, for example, is an order of magnitude lower than the others. This can represent, for instance, how the human knows that the third object is a friendly entity and does not pose much risk besides a potential crash. We assume the human provides the exact value of the gradient information and focus on how we can apply the results in this paper to accommodate the constraints in human performance, as discussed in Section 4.

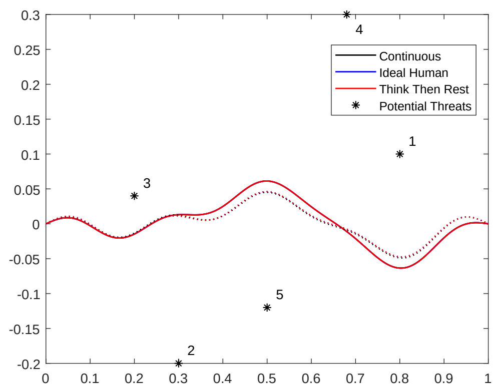

Fig. 2. Optimized trajectories. The diagram shows the trajectories of the optimized amplitudes after 10000 robot iterations with the initial condition of a straight path, $a = 0$. Shown in the dotted lines are the trajectories at 5000 robot iterations for each respective model. The proposed triggers for updating human gradient information shows convergence towards the desired (continuous case) trajectory in all the cases.

We run our simulations in MATLAB on a desktop with a 3.5GHz Intel Core i5-6600K quad-core CPU and 16GB of RAM. For comparison, we generate a reference optimized trajectory having the robot use gradient information at all times. We refer to this as the "continuous" case. To simulate the continuous dynamics, we use an Euler discretization with a stepsize of 1×10^{-5}. Note that the timescales of the robot, over which the dynamics runs, and of the human are not necessarily the same, cf. Remark 4.10. In fact, in our platform, each iteration of this discretization takes the robot roughly one second to compute. Therefore, continuous queries by the robot would mean that the human needs to respond every second. From an operational point of view, this amount of time can be too little for the human to work with. Instead, the results of this paper allow the robot to efficiently query the human in an opportunistic fashion to continue its operation and also allow the human to gain more time to work between consecutive queries.

Even though the resulting optimization problem is not convex, we employ our event-triggered law (4) with $\sigma = 0.5$ to find a local optimizer via human-robot interactive gradient descent (cf. Remark 3.5). Under the ideal human model of Section 3, the trajectory from the resulting optimized amplitudes after 10000 iterations is plotted in Figure 2. Using (11), the lower bound to the interexecution time is 5.2×10^{-4}, i.e., 52 robot iterations. As a result, the human does not need to respond at every iteration to ensure convergence to the desired trajectory. In addition, Figure 3 shows the number of iterations elapsed before the human responds, which is lower bounded by the aforementioned value. Note that the optimal trajectory ends up closer to the obstacle on the left, compared to others. This is expected because the object corresponds to the threat location with weight q_3, which has lower potential risk than the others.

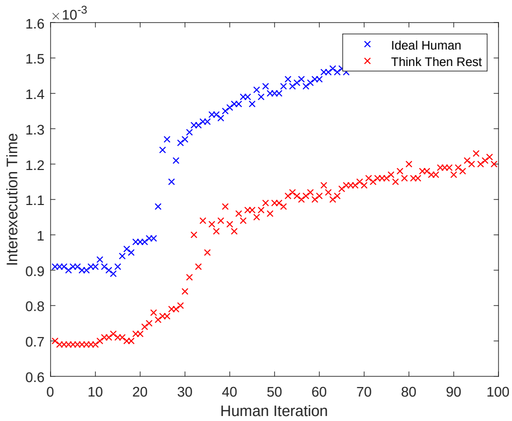

Fig. 3. Interexecution times. The diagram shows the time elapsed between each request from the robot to the human to update the gradient value. The interevent times are uniformly lower bounded in both cases, as guaranteed by our analysis. The robot runs its dynamics with stepsize 1×10^{-5}, which means that the human only has to respond after at least 65 iterations.

Next, we consider a scenario where the human may take time to provide gradient information and may need some time to rest between consecutive queries, as described under the "need to think then rest" model of Section 4.3. With the notation of that section, we select $T_{\text{thk}} = 5 \times 10^{-5}$, which corresponds to 5 robot iterations – i.e., the robot has to wait for up to 5 iterations in the execution of its gradient dynamics before receiving a response from the human to its query. In order to determine the allowable resting times in this scenario, we use (28) from Proposition 4.9 to plot in Figure 4 the design space of pairs $(\sigma, T_{\text{rest}})$ for which the above thinking time D is feasible. To obtain the same guaranteed convergence rate as in the ideal human case, we select $\sigma = 0.5$ and then, based on Figure 4, we pick $T_{\text{rest}} = 1 \times 10^{-4}$ to be in the interior of the feasible option.

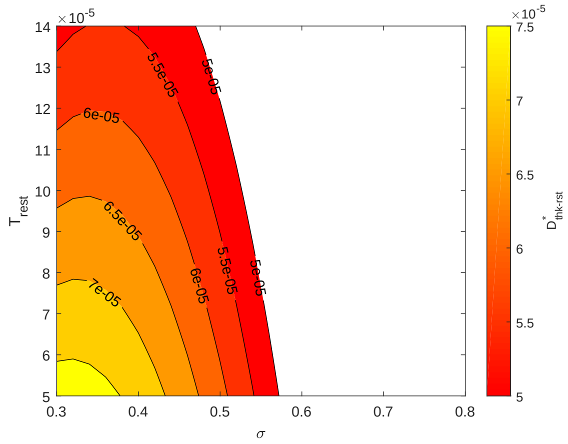

Fig. 4. Design space for "need to think then rest human." The diagram shows the region where the pairs $(\sigma, T_{\text{rest}})$ that can accommodate the thinking time $T_{\text{thk}} = 5 \times 10^{-5}$. The colored region represents the sublevel sets of maximum allowable thinking time $D^*_{\text{tnk-rst}}$, starting with $D^*_{\text{tnk-rst}} \geq 5 \times 10^{-5}$, and the brightness denotes higher values.

Note that this selection corresponds to 10 iterations of the robot. In practice, the algorithm might still converge with much longer resting times because of the various bounds involved in obtaining our guarantee. In fact, in our simulations, cf. Figure 3, we observe that the human actually has the minimum resting time of 6.5×10^{-4}, which corresponds to 65 iterations. According to Proposition 4.9, we select $\sigma' = 0.42$ to satisfy the hypotheses and implement the event-triggered law (24). The result shows that the resting and thinking time constraints are respected and, as expected, the interevent times are reduced to accommodate the delay, cf. Figure 3. Figure 5 shows the evolution of the Lyapunov function, where one can see that the same level of performance as in the ideal human case is attained.

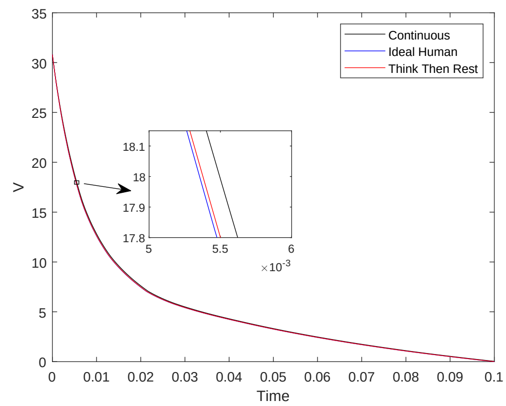

Fig. 5. Convergence of the cost function. The plot shows the evolution of the Lyapunov function using our event-triggered design for different models. The design parameters σ for the "need to think then rest" model is chosen to match the convergence guarantee of the ideal human case.

6 Conclusions

We have developed event-triggered strategies for human-robot interactive multiobjective optimization. Our design seeks to minimize human workload by having the robot require her involvement in an opportunistic fashion when it is necessary to ensure the asymptotic correctness of the robot dynamics. We have shown how different human performance limitations can be accommodated, such as the human requiring some time between consecutive queries, requiring some time before producing a response, and a combination thereof. For each model, we show that the corresponding event-triggered strategy is provably correct and Zeno-free, with uniformly lower bounded inter-event times. We believe further work could expand the versatility and flexibility of the proposed solutions, including improving upon the conservatism of our proposed designs. In particular, we will seek to extend our designs here beyond gradient dynamics to incorporate other optimization methods, explore the online learning of human models with the information received by the robot to reduce the workload, expand upon the use of the concept of grace time and the idea of allowing controlled increases of the Lyapunov function along the system trajectories, and the incorporation of time-varying human preference functions and inexact human responses to robot queries.

References

J. W. Crandall, M. A. Goodrich, Jr. D. R. Olsen, and C. W. Nielsen. Validating human-robot interaction schemes in multitasking environments. *IEEE Transactions on Systems, Man & Cybernetics. Part A: Systems & Humans*, 35(4):438–449, 2005.

G. Debreu. Representation of a preference ordering by a numerical function. *Decision processes*, 3:159–165, 1954.

V. S. Dolk, D. P. Borgers, and W. P. M. H. Heemels. Dynamic event-triggered control: Tradeoffs between transmission intervals and performance. In *IEEE Conf. on Decision and Control*, pages 2764–2769, Los Angeles, CA, December 2014.

V. S. Dolk, D. P. Borgers, and W. P. M. H. Heemels. Output-based and decentralized dynamic event-triggered control with guaranteed $\mathcal{L}_p$-gain performance and Zeno-freeness. *IEEE Transactions on Automatic Control*, 62(1):34–49, 2017.

A. M. Geoffrion, J. S. Dyer, and A. Feinberg. An interactive approach for multi-criterion optimization, with an application to the operation of an academic department. *Management Science*, 19(4-part-1):357–368, 1972.

A. Girard. Dynamic triggering mechanisms for event-triggered control. *IEEE Transactions on Automatic Control*, 60:1992–1997, 2015.

M. A. Goodrich and A. C. Schultz. Human-robot interaction: A survey. *Foundations and Trends in Human-Computer Interaction*, 1(3):203–275, 2007.

C. E. Harriott and J. A. Adams. Towards reaction and response time metrics for real-world human-robot interaction. In *IEEE International Symposium on Robot and Human Interactive Communication (RO-MAN)*, pages 799–804, Aug 2017.

W. P. M. H. Heemels, K. H. Johansson, and P. Tabuada. An introduction to event-triggered and self-triggered control. In *IEEE Conf. on Decision and Control*, pages 3270–3285, Maui, HI, 2012.

L. Hetel, J. Daafouz, and C. Iung. Stabilization of arbitrary switched linear systems with unknown time-varying delays. *IEEE Transactions on Automatic Control*, 51(10):1668–1674, Oct 2006.

H. K. Khalil. *Nonlinear Systems*. Prentice Hall, 3 edition, 2002. ISBN 0130673897.

S. S. Kia, J. Cortés, and S. Martinez. Distributed convex optimization via continuous-time coordination algorithms with discrete-time communication. *Automatica*, 55:254–264, 2015.

L. Li, X. Wang, and M. D. Lemmon. Stabilizing bit-rate of disturbed event triggered control systems. In *Proceedings of the 4th IFAC Conference on Analysis and Design of Hybrid Systems*, pages 70–75, Eindhoven, Netherlands, June 2012.

M. Luque, J. B. Yang, and B. Y. H. Wong. Project method for multiobjective optimization based on gradient projection and reference points. *IEEE Transactions on Systems, Man & Cybernetics. Part A: Systems & Humans*, 39(4):864–879, 2009.

K. Miettinen, F. Ruiz, and A. P. Wierzbicki. Introduction to multiobjective optimization: Interactive approaches. In Jürgen Branke, Kalyanmoy Deb, Kaisa Miettinen, and Roman Słowiński, editors, *Multiobjective Optimization: Interactive and Evolutionary Approaches*, pages 27–57. Springer, Berlin, Heidelberg, 2008.

M. Miskowicz. *Event-Based Control and Signal Processing*. CRC Press, 2015. ISBN 9781482256550.

P. Ong and J. Cortés. Event-triggered interactive gradient descent for real-time multi-objective optimization. In *IEEE Conf. on Decision and Control*, pages 5445–5450, Melbourne, Australia, December 2017.

P. Ong and J. Cortés. Event-triggered control design with performance barrier. In *IEEE Conf. on Decision and Control*, pages 951–956, Miami Beach, FL, December 2018.

S. Peitz and M. Dellnitz. A survey of recent trends in multiobjective optimal control – surrogate models, feedback control and objective reduction. *Mathematical and Computational Applications*, 23, June 2018.

S. Peitz, K. Schfer, S. Ober-Blbaum, J. Eckstein, U. Khler, and M. Dellnitz. A multiobjective MPC approach for autonomously driven electric vehicles. *IFAC-PapersOnLine*, 50 (1):8674 – 8679, 2017.

J. R. Peters, V. Srivastava, G. S. Taylor, A. Surana, M. P. Eckstein, and F. Bullo. Human supervisory control of robotic teams: Integrating cognitive modeling with engineering design. *IEEE Control Systems*, 35(6):57–80, 2015.

D. Richert and J. Cortés. Distributed linear programming with event-triggered communication. *SIAM Journal on Control and Optimization*, 54(3):1769–1797, 2016.

M. Sakawa. Interactive multiobjective decision making by the sequential proxy optimization technique: SPOT. *European Journal of Operational Research*, 9(4):386–396, 1982.

M. T. Shaikh and M. A. Goodrich. Design and evaluation of adverb palette: A GUI for selecting tradeoffs in multi-objective optimization problems. In *ACM/IEEE International Conference on Human-Robot Interaction (HRI)*, pages 389–397, March 2017.

A. Steinfeld, T. Fong, D. B. Kaber, M. Lewis, J. Scholtz, A. C. Schultz, and M. A. Goodrich. Common metrics for human-robot interaction. In *HRI*, pages 33–40, Salt Lake City, Utah, USA, March 2006.

P. Tabuada. Event-triggered real-time scheduling of stabilizing control tasks. *IEEE Transactions on Automatic Control*, 52 (9):1680–1685, 2007.

X. Wang and M. D. Lemmon. Event-triggering in distributed networked control systems. *IEEE Transactions on Automatic Control*, 56(3):586–601, 2011.

J. Weimer, J. Araújo, and K. H. Johansson. Distributed event-triggered estimation in networked systems. *IFAC Proceedings Volumes*, 45(9):178–185, 2012.

W. Wu, S. Reimann, D. Görges, and S. Liu. Suboptimal event-triggered control for time-delayed linear systems. *IEEE Transactions on Automatic Control*, 60(5):1386–1391, May 2015.

B. Xin, L. Chen, J. Chen, H. Ishibuchi, K. Hirota, and B. Liu. Interactive multiobjective optimization: A review of the state-of-the-art. *IEEE Access*, 6:41256–41279, 2018.

J. B. Yang. Gradient projection and local region search for multiobjective optimisation. *European Journal of Operational Research*, 112(2):432–459, 1999.